RESEARCH ARTICLE | JUNE 27 2017

Atmospheric transmission loss in mirror-to-tower slant ranges due to water vapor FREE

Christian A. Gueymard; Gabriel López; Igor Rapp-Arrarás

AIP Conf. Proc. 1850, 140010 (2017)
https://doi.org/10.1063/1.4984518

Atmospheric Transmission Loss in Mirror-To-Tower Slant Ranges Due to Water Vapor

Christian A. Gueymard[1, a)], Gabriel López[2, b)], Igor Rapp-Arrarás[3, c)]

[1]*Solar Consulting Services, P.O. Box 392, Colebrook, NH 03576 USA.*
[2]*Dpto. Ingeniería Eléctrica y Térmica, de Diseño y Proyectos, ETSI, Universidad de Huelva, Ctra. Palos de la Frontera s/n, 21819 Palos de la Frontera, Huelva, Spain.*
[3]*Dpto. Ciencias Agroforestales, ETSI, Universidad de Huelva, Ctra. Palos de la Frontera s/n, 21819 Palos de la Frontera, Huelva, Spain.*

[a)]Corresponding author: chris@solarconsultingservices.com
[b)]gabriel.lopez@die.uhu.es
[b)]igor@dcaf.uhu.es

Abstract. Considering CSP systems of the central tower-receiver type, this study investigates the specific effect of water vapor absorption on the total atmospheric transmission losses that impact direct irradiance along the slant path between a distant mirror and the receiver on the tower. Spectral and broadband calculations of total atmospheric attenuation are made for various water vapor conditions (from dry to humid) with both the rigorous MODTRAN code and the simpler and faster SMARTS code. The use of the latter is made indirectly possible through the "fictitious sun" concept. The MODTRAN and SMARTS results compare reasonably well under the present conditions, which closely echo the conditions used in previous studies, thus allowing instructive comparisons that will be reported later. To study the vertical profile of water vapor between surface and a height of 300 m, the columnar precipitable water at ≈5 m resolution has been derived from special high-resolution radiosonde soundings carried out twice daily at two arid sites. This analysis shows that the desired precipitable water at the receiver level can be simply extrapolated from that at the mirror level if the water vapor scale height is known. The latter is shown to significantly vary on a daily basis at the two sounding sites, with a median of 2.74 km. The exact value of this scale height conditions the transmission loss due to water vapor, but in any case this loss is found relatively small in comparison with other sources of attenuation, even when considering long slant paths under humid conditions. This unexpected finding is explained by the saturation effect that characterizes water vapor absorption.

INTRODUCTION

Concentrating Solar Power (CSP) systems using the concept of a central receiver on top of a tower were successfully developed in the early 1970s. A seminal study [1] from that period showed that, for such designs, an important factor to take into account is the attenuation of the incident direct normal irradiance (DNI) along the mirror-to-tower slant path. The initial calculations in [1] were made for mirror-to-tower slant ranges of up to 2 km, and showed that the propagation loss could be substantial, depending on local visibility conditions. A resurgence of studies on this topic has occurred recently. Some of them tackle the problem experimentally, whereas most of them follow a methodology similar to that in [1] (e.g., [2]), however using the MODTRAN atmospheric code [3], which replaced the older LOWTRAN used in [1]. Alternatively, a substantially simplified (broadband-only) approach has also been recently proposed [4]. Whereas, in general, most studies are concerned with only the propagation loss in broadband DNI, it has been shown that spectral information could be useful too [2, 5]. The present investigation uses two modeling approaches of differing complexity to quantify the specific effect of water vapor absorption, while retaining the added value offered by the underlying spectral information. Up to now, the main focus of the existing literature has been on the impact of aerosols, which tend to concentrate in the bottom layer of the

SolarPACES 2016
AIP Conf. Proc. 1850, 140010-1–140010-7; doi: 10.1063/1.4984518
Published by AIP Publishing. 978-0-7354-1522-5/$30.00

atmosphere. To generalize these results, however, it is also important to evaluate the additional impact of water vapor, which is also concentrated in the lower atmosphere, but attenuates radiation in a different part of the spectrum than aerosols. There currently exists no specific data on the quantity of water vapor contained in the bottom layer of the atmosphere from surface to a height of up to 300 m (representative of the tallest central towers being envisioned). The quantification of this variable and of the resulting water vapor effect on slant transmission loss is specifically examined in what follows.

METHODOLOGY

A first series of calculations is done here using the conventional slant propagation approach that considers the extinction between two points in the atmosphere (mirror and tower's receiver) after the direct beam has been attenuated along its atmospheric path down to the mirror. This is performed here with the MODTRAN code, which can provide high-resolution spectral information. The procedure's schematic is shown in Fig. 1. The irradiance incident on mirror M, E_M, is reflected then attenuated between M and the tower T, so that the irradiance at T is E_T with

$$E_T = R\,(1-A)\,E_M \tag{1}$$

where R is the total mirror's reflectance and A is the atmospheric transmission loss between M and T. In this preliminary work, and for the sake of simplicity, the total mirror's reflectance is simply set to 100%. The irradiance incident on the mirror is given by MODTRAN as:

$$E_M = \int_{0.28\,\mu m}^{4\,\mu m} T_{\lambda M} E_{\lambda 0}\, d\lambda \tag{2}$$

where $E_{\lambda 0}$ is the Kurucz extraterrestrial spectral irradiance at 1 AU, and $T_{\lambda M}$ is the atmospheric spectral transmittance for the sun-to-mirror path, which depends on the abundance of various atmospheric constituents, and thus varies over time. The integration limits correspond to the range of wavelengths (λ) typically sensed by a pyrheliometer. Since only the attenuation due to water vapor is specifically evaluated here, all other inputs (including aerosols) are fixed to reasonable values. In this regard, the atmospheric profile and total column amounts of atmospheric constituents are those specified by the 1976 US Standard Atmosphere (USSA), except for carbon dioxide, which is set to the more current value of 400 ppmv. The selected aerosol model corresponds to the Rural extinction profile with a meteorological range of 23 km at mirror level. This selection of atmospheric conditions reflects what has been done in previous studies, thus allowing direct comparisons. The solar zenith angle is set to 30º, which yields an airmass of ≈1.155. Although different solar positions lead to different transmission losses, the effect of varying solar position is analyzed in a separate contribution. The irradiance reaching the tower's receiver is obtained using MODTRAN's slant path option for two points at finite distance, i.e., the mirror and the receiver. The irradiance incident on the latter, E_T, is then such that:

$$E_T = \int_{0.28\,\mu m}^{4\,\mu m} \rho_\lambda T_{\lambda M-T} E_{\lambda M}\, d\lambda \tag{3}$$

where ρ_λ is the mirror spectral reflectance (which is set here to 1 as noted above), $E_{\lambda M}$ is the spectral irradiance incident on the mirror, and $T_{\lambda M\text{-}T}$ is the spectral transmittance for the mirror-to-tower slant path. The loss due to atmospheric attenuation, A, may then be derived by solving Eqs. (1–3).

The general procedure just described has drawbacks, however. In particular, the MODTRAN code is complex, not in the public domain, not oriented toward solar applications, and may require specific inputs that are difficult to obtain in practice if accurate and localized simulations are desired. Clearly, an alternative model tailored for solar applications would be desirable.

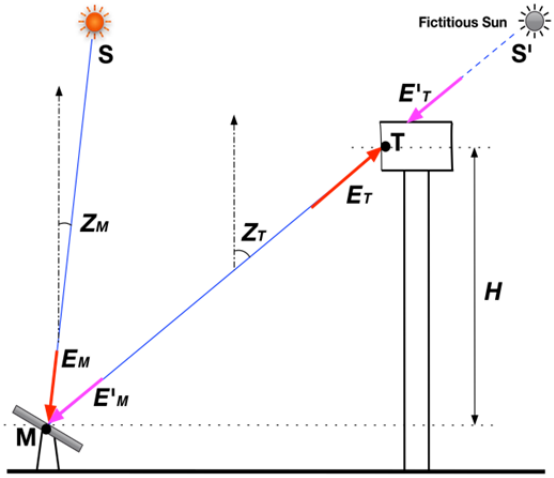

FIGURE 1. Irradiances scheme for calculating atmospheric transmission loss in mirror-to-tower paths. Also shown are the irradiances E'_M and E'_T and the zenith angle Z_T pertaining to the fictitious sun method.

The alternate method developed here is considerably simpler than that based on MODTRAN and is based on the "fictitious sun" concept, which is schematized in Fig. 1. It can accommodate either spectral calculations using, e.g., the SMARTS code [6, 7], which is much easier and faster than MODTRAN, or direct broadband calculations using, e.g., the REST2 clear-sky radiation model [8]. As the literature shows, it is possible to evaluate *A if* the main radiative characteristics of the atmosphere are known *between M and T*. That path determination is the difficult part of the direct method, and the reason why its analysis requires a sophisticated model such as MODTRAN. The alternate method introduced here (Fig. 1) is indirect and rather considers a fictitious sun at S', in the alignment of M and T. The fictitious irradiances at M and T are E'_M and E'_T, respectively. The desired M-T transmission loss is then simply $A = 1 - E'_M / E'_T$. Separate evaluations of E'_M and E'_T are done using a procedure similar to that above, per Eqs. (2) and (3).

Figure 2 shows the atmospheric spectral transmittance for a slant mirror-to-tower path corresponding to a receiver height H = 100 m, a slant range R = 2 km, and precipitable water columnar amount at mirror level w = 1.42 cm (as prescribed by USSA). The two methods agree reasonably well, considering the lower resolution of SMARTS compared to MODTRAN, and differences in their respective extraterrestrial spectra, in particular. The total DNI reaching the tower after ideal reflection by the mirror is 600 W/m^2 when using MODTRAN and 608 W/m^2 when using SMARTS, which is a reasonable agreement owing to the differences just mentioned. Since the modeled DNI incident onto the mirror is 785 W/m^2 under the present conditions, overall losses of 23.6% and 22.5% are obtained for this specific geometry, respectively for the two methodologies.

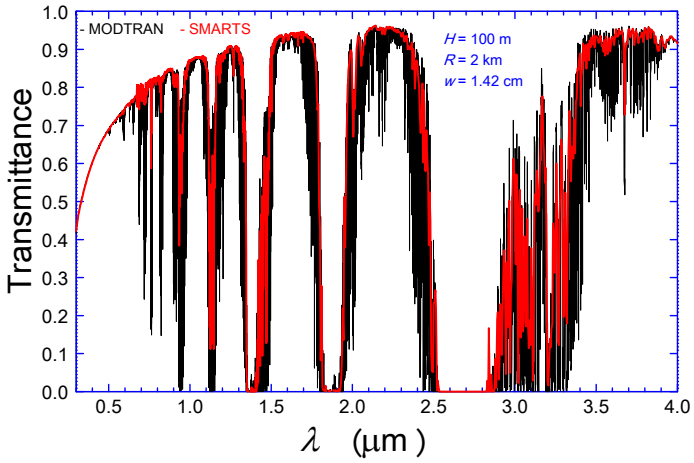

FIGURE 2. Spectral transmittance comparison for the slant path mirror-to-tower using MODTRAN and the simpler 'sun fictitious method' with SMARTS.

ATMOSPHERIC WATER VAPOR PROFILES

It is assumed here that the atmospheric conditions are known at the surface (mirror level), most particularly precipitable water (w) and pressure (p). The former can be easily obtained from various sources of data, such as radiosonde, GPS, sunphotometer, satellite or reanalysis [9]. The conditions at the receiver are typically not known, however, and thus must be extrapolated from those at the surface. The change in p is just a simple function of the tower's height H. The difficulty here is that there is little readily available information about the vertical profiles of w between the surface and an altitude of 100–300 m. Fortunately, an analysis of the vertical profile of w in that layer can be done using high-resolution radiosonde soundings from, e.g., the SPARC database [10]. Their 1-second temporal resolution translates into a vertical resolution of ≈5 m close to the ground, which is enough for the present application. At each level during the ascent, the columnar water vapor can be derived from three variables (temperature, relative humidity and pressure) that are measured at each level of observation by the radiosonde. The numerical integration procedure is adapted from that in [11]. An example of one year of twice-daily profiles at two SPARC stations in arid environments is shown in Fig. 3. To reduce the data, it is convenient to use the concept of *scale height* [12], which describes the rapid vertical decrease in water vapor with an exponential function of elevation. The annual average scale height between surface and a height of 300 m, H_w, at the two sites confounded is ≈2.8 km. This is comparable to the value of 2.5 km suggested for the whole-column scale height of inland sites in an earlier study [12], which used completely different sources of data. Moreover, note that the scale height defined here between 0 and 300 m tends to be systematically different from that between 0 and the top of the vertical water vapor column, which was considered in the earlier study. For instance, the mean scale height at the two SPARC sites under scrutiny is only ≈2.1 km when evaluated over the whole vertical column.

For H below 300 m, it is easy to derive $w(H)$ at height H (receiver) from $w(0)$ at ground level (mirror) using

$$w(H) = w(0)e^{-\frac{H}{H_w}} \approx w(0)\left(1-\frac{H}{H_w}\right) \tag{4}$$

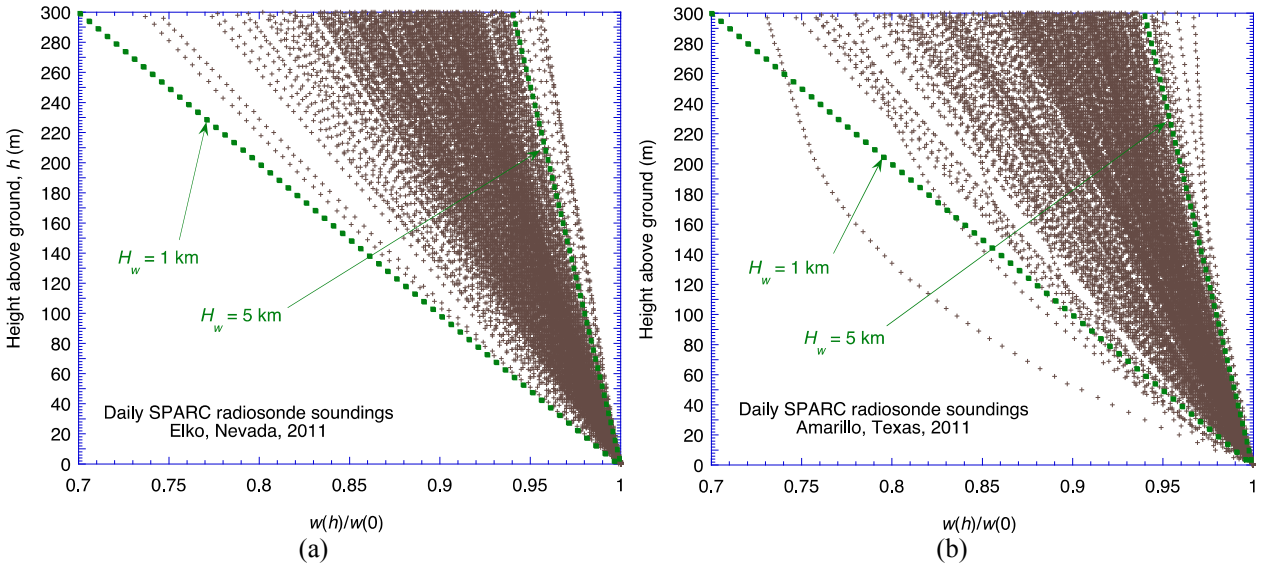

FIGURE 3. Variation of precipitable water, w, with height above surface at Elko, NV (a) and Amarillo, TX (b) using high-resolution radiosonde soundings. Each derived value of normalized columnar w is shown with a + symbol.

Equation (4) implies that, for H = 200 m and H_w = 2 km, for instance, as much as 10% of the total water vapor column lies *below* the receiver, which is significant. Figure 3 shows that H_w can vary significantly over time, due to rapid natural changes in weather conditions. It also varies on a site-by-site basis, due to differing climatic conditions. In the vast majority of cases (95%) for the stations under scrutiny here, scale heights are within the 1.5–4.9 km range. More specifically, Fig. 4 shows the corresponding frequency distribution of H_w in the 0–300 m near-surface layer. This distribution is apparently more log-normal than Gaussian, with a median value of 2.74 km.

Note that the SPARC stations under scrutiny here are in warm regions, with only occasional cold periods. When the temperature near the ground gets cold, temperature inversions become frequent, thus disrupting the linearity of vertical profiles [13], compared to those shown in Fig. 3. Hence, such cases would require specific attention if CSP-tower projects were to be built in cold areas. Cold temperatures tend to increase H_w to values much larger than 3 km, which explains the long tail of the distribution in Fig. 4.

The analysis above, based on actual high-resolution observations, provides a much larger range of information about real conditions than what can be normally described in MODTRAN or similar atmospheric tools. This is because the few atmosphere models that can be selected in them have a vertical resolution of only 1 km close to the surface, and just have a single fixed vertical profile for each constituent, which is internally linearly interpolated at run time to define local properties at any height. Based on the MODTRAN data compiled in [7], Table 1 provides the mean 0–1-km scale height of the six selectable atmosphere models it offers. All of them, except the SAW atmosphere, can only emulate the average conditions that are observed at the two SPARC sites. (The larger value of H_w under SAW corresponds to a very cold surface temperature of -16°C and a slight inversion at a height of ≈1 km [13].) The discussion above means that MODTRAN would not be useful to evaluate the transmission loss due to water vapor under near-extreme H_w conditions, for instance, unless actual soundings are provided as an input, which complicates its usage even more.

TABLE 1. Water vapor scale height between surface and a height of 1 km for six atmosphere models selectable in MODTRAN. The surface temperature assumed by each model is also indicated.

Atmosphere	H_w (km)	T (°C)	Atmosphere	H_w (km)	T (°C)
U.S. Standard Atmos. (USSA)	2.729	15.0	Sub-Arctic Summer (SAS)	2.725	14.0
Mid-Latitude Summer (MLS)	2.439	21.0	Sub-Arctic Winter (SAW)	3.287	-16.0
Mid-Latitude Winter (MLW)	2.794	-1.0	Tropical	2.537	26.5

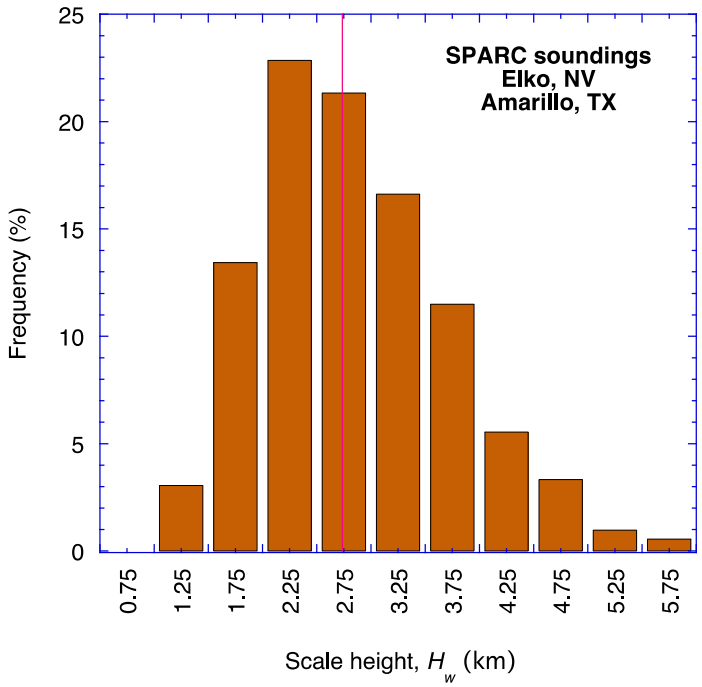

FIGURE 4. Frequency distribution of the near-surface water vapor scale height at two SPARC radiosonde stations, based on one year of twice-daily soundings at each site. The vertical red line indicates the median value (2.74 km).

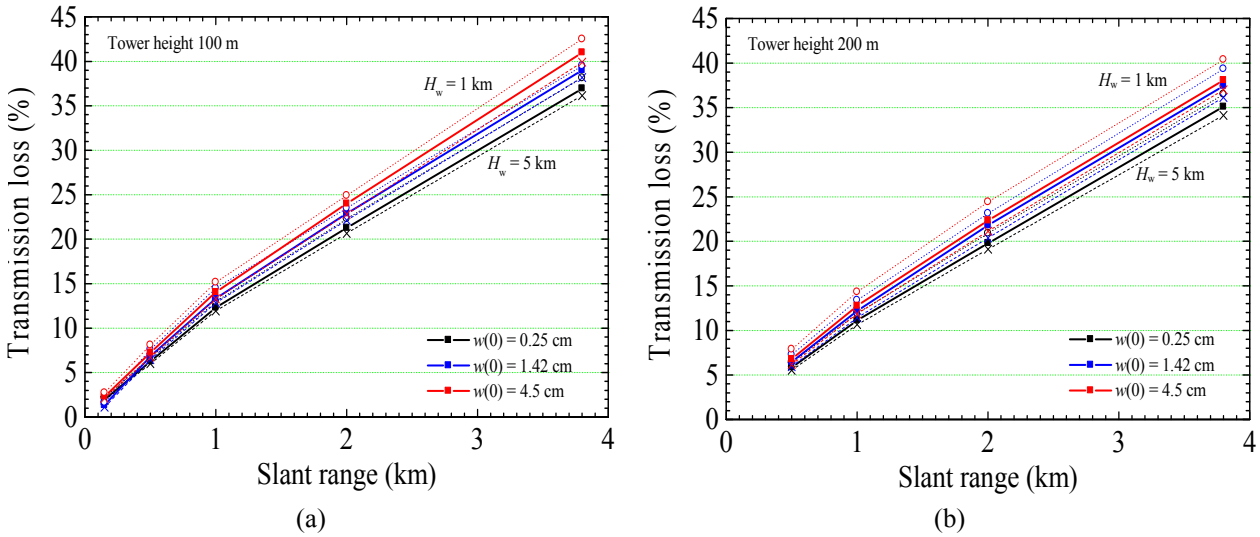

FIGURE 5. Total atmospheric transmission loss for (a) H = 100 m and (b) H = 200 m using SMARTS and 3 representative values of w for dry (0.25 cm), average (1.42 cm), and humid (4.5 cm) conditions. Average results (thick curves) are for H_w = 2.1 km. Extreme results (thin dashed curves) are for H_w = 1 or 5 km.

RESULTS

The variables investigated here are H, H_w, w, and the slant range, R. The latter is varied between 0.15 and 3.8 km to allow comparisons with previous estimates from, e.g., [1, 2]. The total transmission loss is shown in Fig. 5 for various water vapor conditions, and separately for H = 100 and 200 m. In both cases, the transmission loss due to water vapor is found relatively small, even under very humid conditions ($w(0)$ = 4.5 cm), in comparison with aerosol-induced losses. These are presumably on the high side here, however, due to the assumed aerosol regime (23-km meteorological range), which corresponds to somewhat hazy conditions. The limited impact of water vapor in all cases studied can be explained by the saturation effect that is specific to the absorption characteristics of that gas, which makes the solar spectrum incident at the mirror already severely depleted inside the water vapor absorption bands, such as around 940 nm or 1400 nm (Fig. 2). The bulk of water vapor absorption occurs before the direct beam reaches the mirror. Any additional water vapor along the mirror-to-receiver path cannot have additional effect on the strongest spectral absorption lines that are already fully saturated, and can only have minimal effect on the moderately strong lines that are almost saturated. Only large amounts of water vapor below the receiver level could potentially have significant effect, but such conditions are unlikely.

The discussion above explains the observation from Fig. 5 that the propagation loss due to water vapor remains almost constant as the slant range R increases from 2 to 3.8 km. This contrasts with the bulk of the attenuation (due to aerosols and molecular scattering), which increases almost linearly with R (Fig. 5).

Interestingly, for the same R, the loss for H = 200 m is slightly lower than for H = 100 m (Fig. 5). This could be expected, however, since for the same slant range, the sun rays are impacted by a larger amount of water vapor and aerosols closer to the ground when the tower is small, compared to a more tilted slant path corresponding to a taller tower. Considering H_w = 2.1 km, the USSA standard value of precipitable water (1.42 cm), and any slant range, the loss decreases by only ≈1.5% as tower height is doubled from 100 m to 200 m.

The effect of the water vapor scale height (H_w) is also evident in Fig. 5. For humid conditions (w = 4.5 cm), a decrease in H_w from 5 km to 1 km leads to a propagation loss increase of about 3%. Scale heights smaller than 1.5 km should be extremely rare, but substantial daily variability can still be expected. For regions where climatic conditions include both humid and dry seasons, a large daily and seasonal variability in H_w can be expected. The propagation loss due to water vapor can then increase by as much as 4 to 6% for slant paths ranging from 0.5 km to 2 km or more, respectively.

CONCLUSIONS

In this study, the attenuation of direct normal irradiance is evaluated along its path from distant mirrors to the tower receiver of a large CSP plant, from the standpoint of the specific impact of water vapor. Two analysis methods are used in parallel. The first method evaluates the mirror-to-receiver attenuation directly through the use of the MODTRAN atmospheric code, thus allowing comparisons with previous results of the literature. The use of MODTRAN being cumbersome for various reasons, an alternate method is devised, based on the "fictitious sun" (FS) concept. This allows the mirror-to-receiver attenuation to be evaluated indirectly from the ratio of sun-to-mirror and sun-to-receiver transmittances. In this case, the SMARTS spectral code is the tool of choice for its speed and ease of use, but other models (including clear-sky broadband models) could be used too.

The transmittance from the fictitious sun to the receiver requires knowledge of the water vapor conditions at the receiver level, which are normally unknown. A specific study of the vertical profile of water vapor close to the ground (between the surface and a height of 300 m) is undertaken here, based on high-resolution radiosonde soundings at two arid sites. This shows that the vertical amount of water vapor at the receiver level can be simply extrapolated from that at the mirror level using an estimate of the water vapor scale height. This is found to vary typically between about 1.5 and 5 km, with a median value of 2.74 km.

The conventional attenuation method based on MODTRAN, as well as the FS method based on SMARTS, are shown to agree reasonably well, considering the various sources of difference in the two codes. An evaluation of the transmission losses induced by water vapor for different cases of slant range (from 0.15 to 3.8 km) and receiver height (100 and 200 m) shows that these losses depend on the scale height and on total precipitable water, but are relatively small anyway in comparison with the total losses. The latter also include the effects of aerosol extinction and Rayleigh scattering. The relatively low impact of water vapor is explained by the saturation effect in water vapor absorption. It is however likely that the relative impact of water vapor can be significantly higher under less hazy conditions when the aerosol-induced attenuation is much less.

Further developments of the FS method are underway to extend its application to cover the general case, where all possible sources of slant transmission losses can be evaluated separately to ease parameterization.

ACKNOWLEDGMENT

The authors are grateful for the financial support provided by Spanish Project ENE2014-433 59454-C3-2-R, which is funded by the Ministerio de Economía y Competitividad and co-financed by the European Regional Development Fund.

REFERENCES

1. C.N. Vittitoe and F. Biggs, "Terrestrial propagation", ASES Solar Diversification Conference Proceedings (Denver, CO, USA, 1978).
2. J. Ballestrín and A. Marzo, Solar Energy **86**, 388–392 (2012).
3. A. Berk, L. S. Bernstein and D. C. Robertson, "MODTRAN: A Moderate Resolution Model for LOWTRAN7", Report GL-TR-89-0122, Air Force Geophysical Laboratory, Hanscom, MA (1989).
4. M. Sengupta and M. J. Wagner, "Impact of aerosols on atmospheric attenuation loss in central receiver systems", SolarPACES Conference Proceedings (Granada, Spain, 2011).
5. C. A. Gueymard, Solar Energy **86**, 1667–1668 (2012).
6. C. A. Gueymard, Solar Energy **71**, 325–346 (2001).
7. C. A. Gueymard, "Simple Model for the Atmospheric Radiative Transfer of Sunshine (SMARTS2), Algorithms and performance assessment". Rep. FSEC-PF-270-95, Florida Solar Energy Center (Cocoa, FL, USA, 1995).
8. C. A. Gueymard, Solar Energy **82**, 272–285 (2008).
9. C. A. Gueymard, Solar Energy **101**, 74–82 (2014).
10. P. T. Love and M. A. Geller, Eos Trans. **93**(35), 337–344 (2012).
11. J. E. Hay, Atmosphere **8**(4), 128–143 (1970).
12. C. A. Gueymard and D. Thevenard, Solar Energy **83**, 1998–2018 (2009).
13. C. A. Gueymard, Solar Energy **53**, 57–71 (1994).